Measurements and simulations of a channel flow powered by plasma actuators

Mark Riherd and Subrata Roy[a)]
Applied Physics Research Group, University of Florida, Gainesville, Florida 32611, USA

(Received 28 May 2012; accepted 31 July 2012; published online 7 September 2012)

Experimental measurements and numerical simulations of a dielectric barrier discharge driven flow inside a finite length channel have been performed. Plasma actuators have been used to impart momentum to the flow in the near wall region, which diffuses throughout the height of the channel as it convects downstream. This momentum addition is found to be of sufficient magnitude to create an unsteady channel flow with exit velocities on the order of 1–3 m/s. Pressure and velocity measurements have been taken in order to quantify the effects of varying the number of symmetrically placed pairs of plasma actuators in the channel and the operating voltage applied to the actuators, showing a monotonic increase with respect to both parameters. Power law relationships have been determined for these measurements with respect to the operating voltage, with exponents of 2.0 for the exit velocity and of 5.6 for the maximum pressure differential. The pressure measurements also suggest that the pressure increase due to each actuator is independent of the bulk flow inside the channel. Numerical predictions also agree with the measured pressure and velocity distributions across the channel. The bulk velocity and pressure measurements allow for efficiency calculations of the plasma channel, which are shown to also fit into a power law relationship with respect to the operating voltage. The data collected show that the efficiency of these devices is low, less than 0.1%, but that it increases with a power law exponent of 4.09 to 4.35 indicating the possibility of using such channel for pumping small flows. © *2012 American Institute of Physics*. [http://dx.doi.org/10.1063/1.4749250]

I. INTRODUCTION

There is a distinct need for small pumps in specialized low speed heat transfer and flow applications. These small scale pumps may be necessary to move fluid, to remove excess heat, or to provide a higher quality flow for test purposes, such as a small scale, low speed wind tunnel. While larger axial and centrifugal pumps and fans are a potential tool for these small applications, they are not necessarily the optimal application of technology.

On the very small scale, electrohydrodynamic, electro-osmotic, and magnetohydrodynamic devices have been shown to be effective micropumps.[1] Dielectric barrier discharge (DBD) actuators are electrohydrodynamic devices that impart momentum to a gas.[2–4] This device uses a strong electric field to weakly ionize the working gas, creating a plasma. The electric field then imparts momentum to these charged particles. Through a collisional process, the charged particles impart momentum to the uncharged particles, creating a bulk flow in the vicinity of the plasma actuator.

Numerical studies performed by Wang and Roy[5] showed that DBD actuators are able to produce a significant level of flow in a micro-geometry. The underlying micro-scale technology for this type of pump has recently been demonstrated by Zito *et al.*,[6] verifying that the thrust density of plasma induced body force increases by orders of magnitude as the size of the devices is decreased. So as these DBD based pumps tend towards smaller dimensions and smaller actuators, the thrust density should increase. Debiasi and Jium-Ming[7] expanded on this pump concept, performing limited experiments with DBD actuators in a larger geometry (on the order of centimeters). That study examined the velocity profiles and mass flow rates seen in the channel as a function of the channel height and voltage.

This study aims to further explore the parameter space of the plasma driven channel flow. Velocity and pressure measurements are presented for a range of operating conditions. Both numerical and experimental results are obtained, which qualitatively agree. In addition to the measurements and computations, a brief explanation of the flow physics is also provided. Furthermore, because the plasma actuators are operated in a closed geometry, the hydrodynamic power can be easily inferred because of these pressure and velocity measurements, which allow for the calculation of the efficiency of the plasma devices driving the flow.

II. MACROSCALE PLASMA PUMPS

Under quiescent conditions and a semi-bounded domain, DBD actuators are known to produce wall jets. These wall jets have been shown to mimic the Glauert wall jet similarity solution sufficiently far downstream of the plasma actuator.[8] The body force created by the plasma actuator entrains fluid from upstream of and above the actuator relative to the wall jet (Fig. 1(a)). This fluid is then convected by the wall jet, which gradually decreases in magnitude while increasing in its height normal to the surface.

However, when the domain of the plasma actuation becomes bounded, such as in a channel flow, the regions from which fluid is entrained are modified (Fig. 1(b)). In the

[a)]Electronic mail: roy@ufl.edu. URL: http://cpdlt.mae.ufl.edu/roy/.

 © 2012 American Institute of Physics

Downloaded 10 Sep 2012 to 128.227.210.184. Redistribution subject to AIP license or copyright; see http://jap.aip.org/about/rights_and_permissions

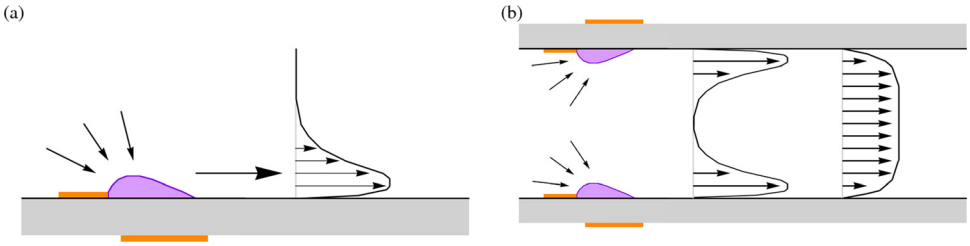

FIG. 1. Comparison of the flow effects for (a) a plasma actuator in a semi-unbounded domain and (b) a pair of oppositely placed plasma actuators in a channel.

bounded domain, the fluid entrained by the wall jet is largely drawn from upstream of the wall jet, though some is still pulled downwards toward the surface. For a pair of plasma actuators placed on opposite sides of a channel, a wall jet will form near both of the actuators. However, as the wall jets expand and decelerate, they will coalesce with each other, eventually forming a channel flow sufficiently far downstream of the plasma actuators. As flow is pushed through the channel, the plasma actuators are effectively acting as a pump or a fan.

This type of pump is fundamentally different from more traditional impeller and positive displacement type pumps.[1] The present pump is largely two dimensional in nature (excepting sidewall effects) and can be extended to any reasonable width to allow for greater mass flux. It also has no rotating parts, or any moving parts at all. As such, the normal metrics for pump characterization (such as the specific speed, $N = n\sqrt{Q}/\Delta p^{0.75}$) may not be applicable.

A number of plasma driven channels, with four sets of single dielectric barrier discharge actuators, have been built for the present experiments, the dimensions of which are shown in Fig. 2(a). The length scales shown are the channel height (h), the distance between the leading edges of two consecutive actuators (s), the total length of the channel (L_1), and the length for the flow to develop downstream of the actuators (L_2). For each plasma actuator, there are also several important length scales (Fig. 2(b)). There are the upper and lower electrode widths (l_T and l_L), as well as the electrode gap (g) and the dielectric thickness (t).

In the experiments performed as part of this study, each plasma actuator is powered by the same high voltage, high frequency signal, and connected to the same electrical ground. All of the plasma actuators have also been built with a uniform electrode geometry, such that they all produce a similar body force. This signal originates in a Tektronics AFG3022B function generator as 14 kHz sinusoidal signal. The signal is then amplified to a higher current using a QSC RMX2450 audio amplifier. A Corona Magnetics high voltage transformer is then used to convert the low voltage, high current signal to a high voltage, low current signal, which is then connected to the powered (upper) electrode. A high voltage probe and oscilloscope are used to measure the signal and ensure that an accurate voltage is applied to the plasma actuators. When a large number of plasma actuators are operated simultaneously (i.e., when the current necessary to power the actuators in the channel exceeds the rating of the transformers), this system is doubled, such that two identical signals originate from the function generator, are amplified, transformed, and connected to the plasma actuators. A diagram of this system is shown in Fig. 3.

The plasma channel was constructed out of PMMA (plexiglass), which also served as the dielectric for the plasma actuators. The grounded electrodes were sandwiched between two layers of PMMA, which were epoxied together. This two layer approach was effective at controlling thermal deformation, which had been significant in earlier experiments where only electrical tape had been used to encapsulate the grounded electrodes. While the DBD actuator creates a "non-thermal" plasma, the actuators still became hot enough to create significant deformations when the channel was not stiffened. Four DBD actuators were installed on the upper surface of the channel and four more were installed on the lower surface of the channel, for a total of eight DBD actuators in the channel. Super glue was used to attach side walls to the channel, allowing for a channel width of 10 cm. The electrodes for the plasma actuators extended all the full width of the channel. While this finite channel width implies that the flow inside the channel is not two dimensional, but is three dimensional instead, with an aspect ratio of 5, this channel should provide a two dimensional flow at the center of the channel's span. Furthermore, measurements were primarily taken at the channel centerline, where the mean flow should be symmetric. For the measurements and simulations performed, a channel of the dimensions listed in Table I.

Before any each set of samples was collected, the plasma actuators were operated for 30 s to remove any transient effects. After each set of samples was collected, the actuators and the channel were allowed to cool down for 180 s. Measurements were performed for a varying number of actuators operated at a single time, and varying the applied voltage for each actuator. As part of this study, the notation of *n* actuators implies that *n* actuators were operated on the upper surface of the plasma channel and *n* more

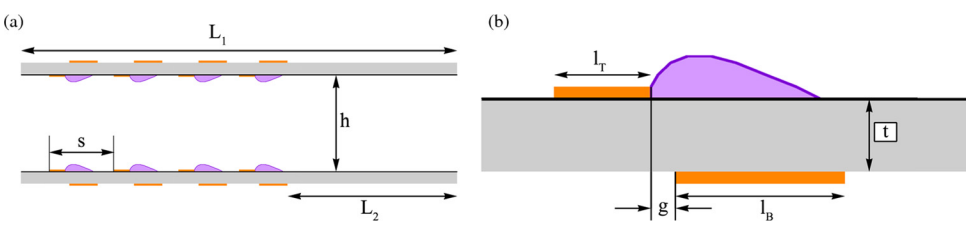

FIG. 2. Diagram of the length scales of (a) the plasma channel and (b) the plasma actuator.

Downloaded 10 Sep 2012 to 128.227.210.184. Redistribution subject to AIP license or copyright; see http://jap.aip.org/about/rights_and_permissions

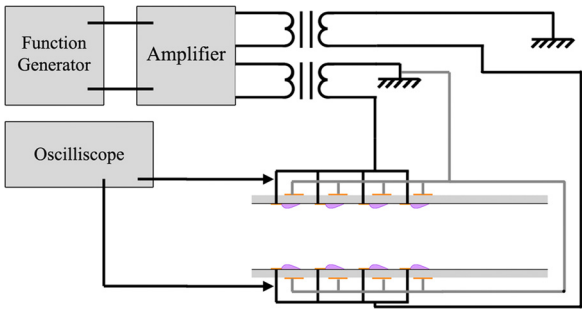

FIG. 3. Circuit diagram of the plasma channel.

actuators were operated on the lower surface in order to promote a symmetric channel flow. These experiments were performed in a 0.6 m × 1.2 m × 1.2 m quiescent chamber. No mean flow was present, except for the flow induced in and around the plasma channel by the DBD actuators. To avoid any confusion, in this study the directions of upstream and downstream refer to the directions up and downstream of the wall jet and channel flow.

While voltage and current data were only observed and not recorded during the collection of velocity and pressure data, electrical data have been collected in order to quantify the amount of power consumption of these actuators during operation. A single actuator of the same dimensions used in the experiments was operated under the same operating conditions as in the experiments. The power data collected show a similar power law relationship as described in recent reviews,[3,4] where power is proportional to $V^{3.5}$ as shown in Fig. 4.

III. VELOCITY MEASUREMENTS

A LaVision Particle Image Velocimetry (PIV) system was used to make measurements of the flow exiting the channel. A 532 nm Nd:YAG laser was used to illuminate the Ondina seeded fluid, as shown in Fig. 5. 250 samples were taken at a rate of 15 samples per second using a Phantom 7.3 high speed camera, which has a 600 × 800 pixel resolution focused on a 4 cm × 5 cm region near the exit of the plasma channel. Measurements inside the channel were attempted,

TABLE I. Dimensions of the plasma channel used for velocity measurements.

Parameter	Value
Channel	
L_t	2.1 cm
L_1	30.0 cm
L_2	20.0 cm
s	2.5 cm
h	2.0 cm
w	10.0 cm
N	1–4
Actuators	
L_T	0.4 cm
L_L	0.4 cm
g	0.0 cm
t	0.25 cm

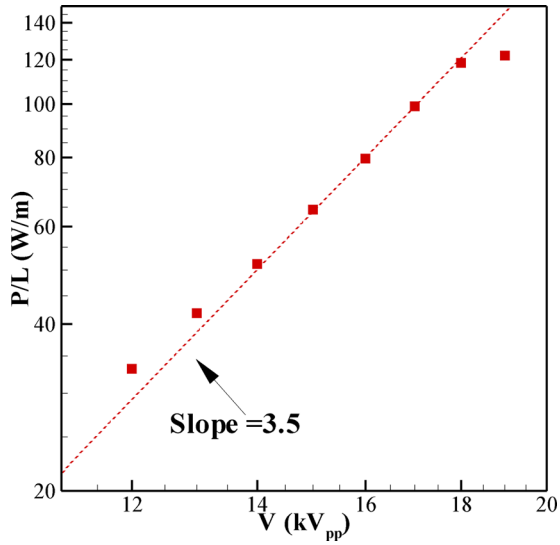

FIG. 4. Power consumption by a single DBD actuator with the same dimensions and dielectric as used in the channel.

but fog from the use of superglue on the channel sidewalls and reflections of the laser bouncing off of the upper and lower channel walls and electrodes prevented high quality from being captured. These samples were then analyzed using LaVision's DAVIS software. The velocity field was calculated using a 16 × 16 pixel integration window with 50% overlap. A 32 × 32 pixel integration window was also used with 50% overlap in order to verify that the results were insensitive to the PIV processing.

It can be seen in Figs. 6(c) and 6(d), that upon its exit, the flow produced by the plasma channel produces unsteady jet-like effects. However, when time averaged over the available samples, the flow can be seen to be nearly symmetric in nature (Figs. 6(a) and 6(b)). These large scale unsteady effects can largely be attributed to instabilities in the jet,[9] rather than large flow perturbations in the channel flow. Based on the exit velocity, the Reynolds number of the channel flow ranges from approximately 1500 to 4000 (for a single set of actuators operated at 16 kV_{pp} to 4 sets of actuators operated at 19 kV_{pp}) in these experiments, which is a range where unsteady effects and hydrodynamic instabilities can become important. While this may lead to a relatively low Reynolds number turbulent channel flow, it does not preclude the channel flow from eventual turbulent flow effects in longer channels with higher Reynolds numbers due to increased flow velocity or channel height.

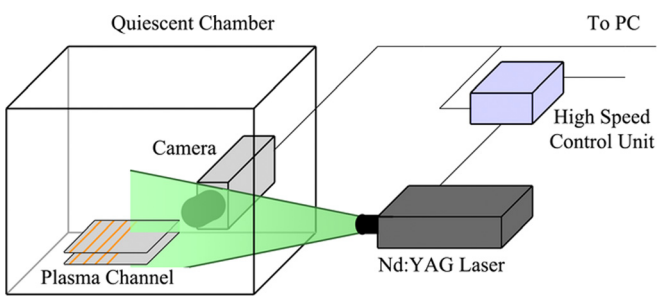

FIG. 5. The PIV setup.

Downloaded 10 Sep 2012 to 128.227.210.184. Redistribution subject to AIP license or copyright; see http://jap.aip.org/about/rights_and_permissions

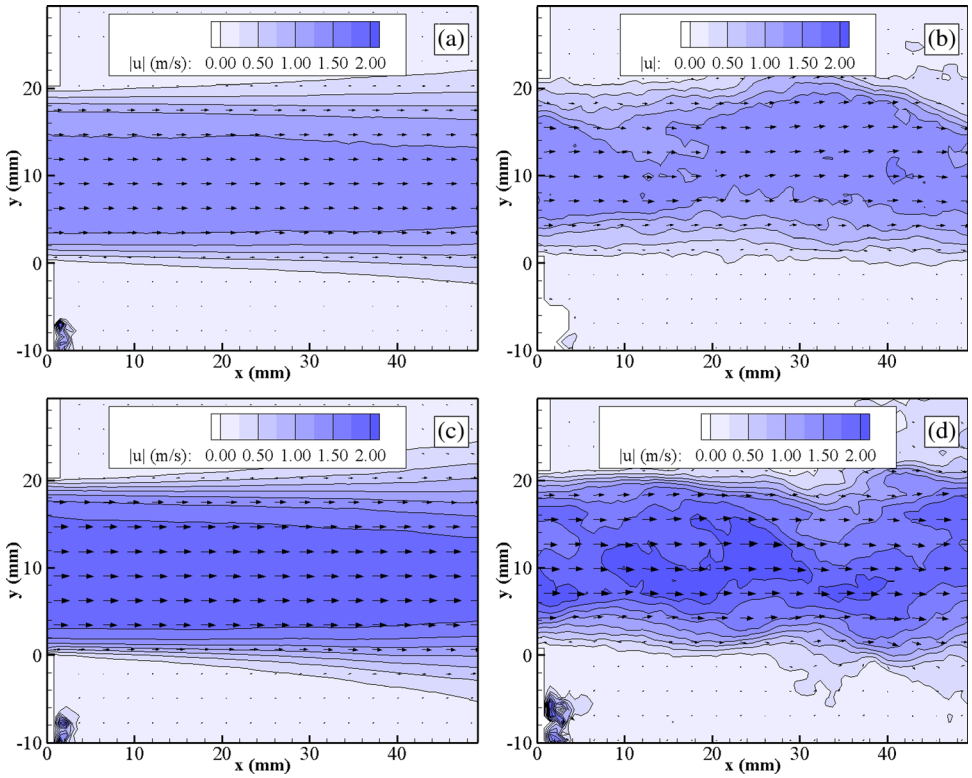

FIG. 6. (a) and (b) Instantaneous and (c) and (d) time averaged velocity magnitudes measurements at the exit of the channel with an applied voltage of 18 kV_{pp} for 1 (a) and (c) and 3 (b) and (d) actuators powered on the top and bottom of the channel.

Exploring the effects of voltage and operating different numbers of plasma actuators simultaneously, it can be seen that the maximum velocity and the total mass flow per unit width ($Q\rho/w$) contained in the channel flow as it exits increases with respect to both the applied voltage and the number of actuators run for a specific case (Fig. 7). This is a logical conclusion to arrive at, as the total amount of body force pushing the fluid downstream increases with respect to both of these variables. As the total amount of body force inside of the channel increases, the momentum addition similarly increases, which will in turn lead to higher velocity flow in the channel. Assuming that a power law relationship can also be applied to the maximum velocity exiting the channel,

$$u_{max} \approx \alpha n_{act}^{\gamma} V^{\beta}. \quad (1)$$

In Eq. (1), n_{act} is the number of pairs of actuators in the channel and α, β, and γ are the empirically derived constants $\alpha = 3.98 \times 10^{-3}$, $\gamma = 0.307$, and $\beta = 2.02$ from a power law curve fit. In this relationship, the voltage, V, must be in kV_{pp}, the maximum velocity in m/s. Performing the same power law curve fit for the mass flow per unit width, the constants are $\alpha = 1.87 \times 10^{-5}$, $\gamma = 0.352$, and $\beta = 2.29$.

The plasma driven channel flow was simulated using a two dimensional version of the implicit large eddy simulation (ILES) code FDL3DI.[10] While this is a compressible Navier-Stokes solver, the present simulations were run at a Mach number of $M = 0.1$ (whereas the actual Mach numbers is approximately $M \sim 0.01$), placing the simulations in the realm of incompressible flow. The plasma body force was implemented through the use of the reduced order model developed by Singh and Roy.[11] Being an approximation of

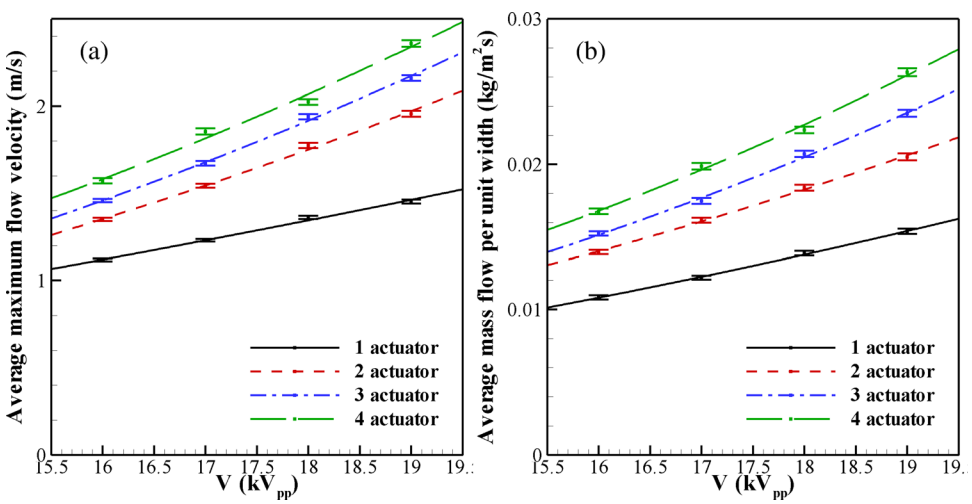

FIG. 7. (a) Maximum velocity and (b) total mass flow per unit width (Qp/w) of the flow 0.5 cm down stream of the channel exit.

Downloaded 10 Sep 2012 to 128.227.210.184. Redistribution subject to AIP license or copyright; see http://jap.aip.org/about/rights_and_permissions

first principle simulation results, it is more accurate that phenomenological models,[12] but not as computationally expensive a first principle simulation.[13,14] The magnitude of the body force was selected such that $D_C = |f_v|h/\rho u_\infty^2$. This level of body force was arbitrarily selected.

A $721 \times 81 \times 55$ (streamwise × height × spanwise) nonuniform mesh was used for the simulations performed. This mesh describes a channel 30 cm in length, 2 cm in height, and 3.75 cm in width. Away from the channel, the mesh extends outwards 25 cm upstream and downstream of the channel and expanding to a height of 14 cm. The mesh was refined near the inlet and outlet of the channel as well as near the channel walls in order to resolve any high gradients that may exist. No slip boundary conditions were applied on the surface of the channel, and no stress conditions applied in the regions up and downstream of the channel. Periodic boundary conditions were applied in the spanwise direction. A Reynolds number of 1333 was selected for normalization based on a velocity of 1 m/s and a channel height of 2 cm.

No turbulence model was implemented, nor was transition induced through the use of external perturbations. As such, beyond the initial transient effects, these simulations provide only a slightly unsteady laminar flow. Furthermore, the plasma actuators were simulated as being flat on the surface, whereas in the experiment, they are applied onto the surface and protrude into the channel approximately 70 μm. These differences between the experiment and simulation are not negligible, and do not allow for a quantitative comparison between experiment and simulation. However, these simulations do allow for a visualization of the effects occurring inside of the plasma channel, which were not of obtainable using PIV and only very coarse data are available in the literature.[7]

The computed velocity fields confirm the coalescing wall jets hypothesis presented in Sec. II. It can be seen in Fig. 8(a) that near the plasma actuator, wall jets are formed on the upper and lower surfaces of the channel. These wall jets grow as they progress downstream, eventually coalescing and forming a channel flow. As the number of actuators increases (Fig. 9), the additional plasma actuators pull the wall jet closer to the wall and increase the maximum velocities seen in the wall jet. However, these additional actuators disrupt the coalescing effects and delay the channel flow from approaching a fully developed state.

It can be seen in Fig. 9 that with the plasma driving the channel near the inlet, there is a uniform flow through the center of the channel. This uniform flow cannot be due to imposed boundary conditions, rather it must be attributed to the manner in which the DBD actuation entrains fluid into the channel. While a uniform flow region was not predicted in Sec. II, it is not surprising. Near the channel inlet, the flow is highly undeveloped. It can be seen that the centerline velocity in the channel increases as the flow moves downstream. This is due to the viscous spreading of the wall jets into the center of the channel, which can be considered a portion of the overall flow development.

IV. PRESSURE MEASUREMENTS

A longer channel ($L_1 = 45$ cm) was also examined in order to better gauge how the pressure varies within the channel around and downstream of the actuators. Pressure taps were installed at numerous locations in the channel. Near the actuators, taps were installed on the side of the channel at the centerline in order to measure the pressure. The centerline location was selected in order to avoid any effects of the wall normal velocity impinging down on the surface of the channel, which could lead to greater uncertainty in the pressure measurements. Downstream of the actuators, where the surface normal velocity induced by the actuators is not of significant concern, pressure taps were installed on the surface of the channel. A Furness Controls Model 332 Differential pressure transmitter was used to take measurements. 512 samples were taken at each location shown at a rate of 20 samples per second. Again, a 30 s warm up period was allowed between the start of plasma actuation and the start of data collection, and a 180 s cool down period after each pressure sampling. The differential pressure was measured against the pressure in the quiescent chamber located approximately 1 m away from the plasma channel. The Thompson-Tau outlier removal method was applied to remove spurious results.

Samples are shown for 1, 2, and 3 plasma actuators running simultaneously. These plasma actuators are located

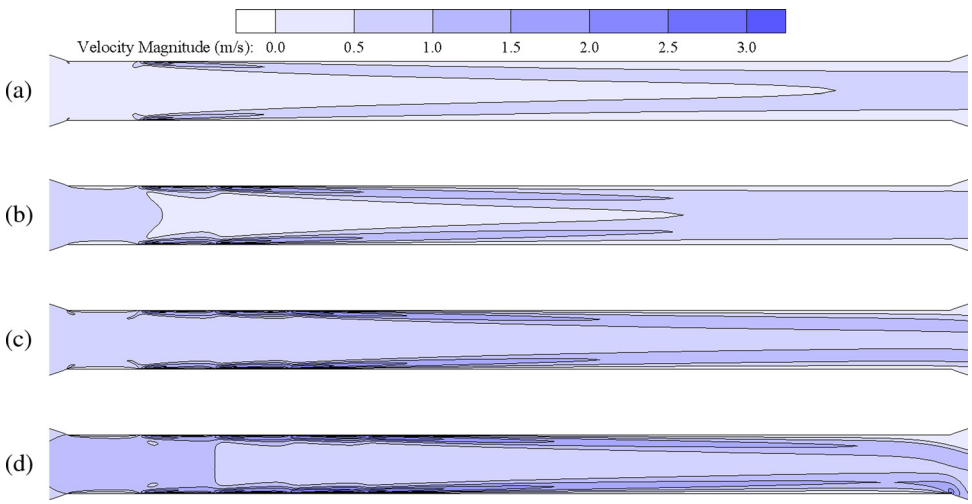

FIG. 8. Instantaneous velocity magnitudes from simulations for (a) 1 actuator, (b) 2 actuators, (c) 3 actuators, and (4) actuators placed symmetrically on the top and bottom of the channel.

Downloaded 10 Sep 2012 to 128.227.210.184. Redistribution subject to AIP license or copyright; see http://jap.aip.org/about/rights_and_permissions

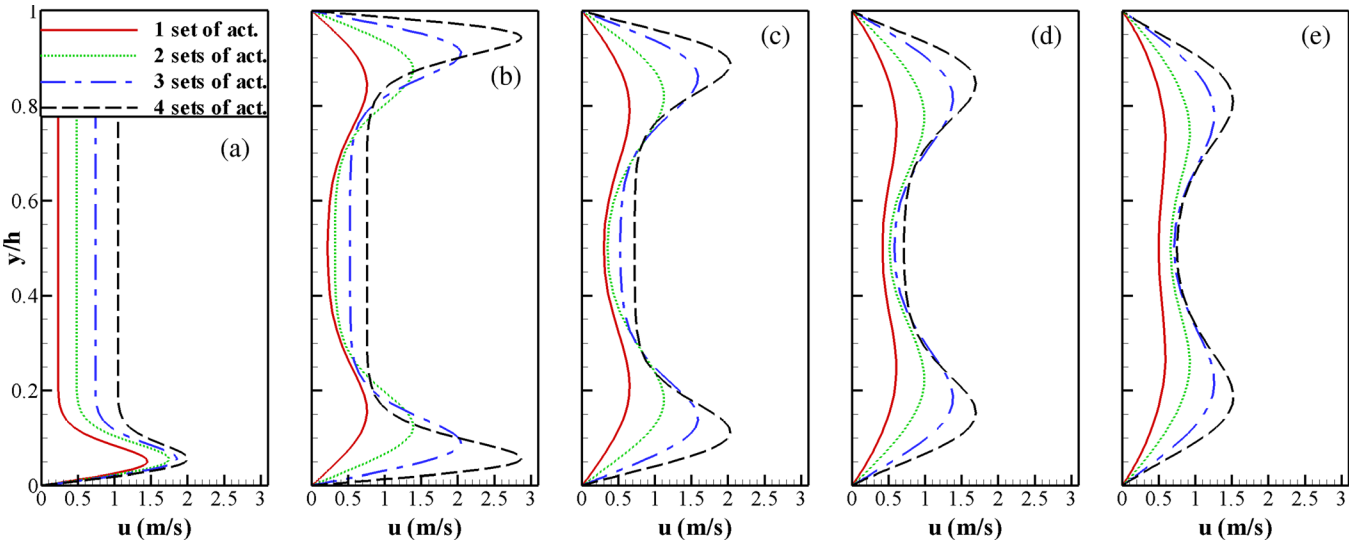

FIG. 9. Simulated velocity profiles within the plasma channel (a) 3.75 cm, (b) 11.25 cm, (c) 16.25 cm, (d) 21.25 cm, and (e) 26.25 cm from the inlet for a varying number of actuators.

between the first and second, second and third, and third and fourth pressure taps. It can be seen in Fig. 10 that there is an initial rise in pressure at the inlet of the channel, corresponding to both the first plasma actuator and any potential inlet effects. With the addition of a second (Fig. 10(b)) and third (Fig. 10(c)) plasma actuator downstream of the initial actuator, further increases in pressure effects can be seen to occur. As one moves downstream of the plasma actuators, the pressure can be seen to continue to increase as the flow develops in the channel. Farther downstream, the pressure is finally seen to slowly drop, indicating that the viscous effects of skin friction with the channel walls create a negative pressure gradient.

Experiments were also performed with a screen impeding the flow of air through the channel downstream of the actuators, with the screen located at x = 15 cm. The screen was approximately 2.5 cm thick, with 3 mm hexagonal holes arranged in a honeycomb pattern. This screen was intended to steady the flow, and remove any vortices in the flow, but the result was a near blockage of flow through the channel. However, pressure measurements were still recorded with the same sampling rate as the unimpeded plasma channel. With this flow impedance, the pressure builds up at the mesh, and the pressure drop in the channel primarily occurs across the mesh, with no significant changes occurring downstream of the mesh (Fig. 11).

While these two channel flow experiments show significant differences in the differential pressure along the length of the channel, when the maximum pressure differential within the interior of the channel is examined (that is $\Delta p_{max} = max(\Delta p) - min(\Delta p)$), a striking result is found (Fig. 12). The maximum pressure differential for the number and applied voltage of the plasma actuators is seen to match up fairly well. This indicates that the plasma actuators are generating the same pressure differential across each actuator, independent of whether the flow is moving downstream or not under these low velocity conditions.

Considering the well behaved nature of these relationships, an empirical model of the expected pressure rise can be developed. A proportional increase in the pressure with respect to the number of plasma actuators employed is expected. Power law relationships have been drawn between

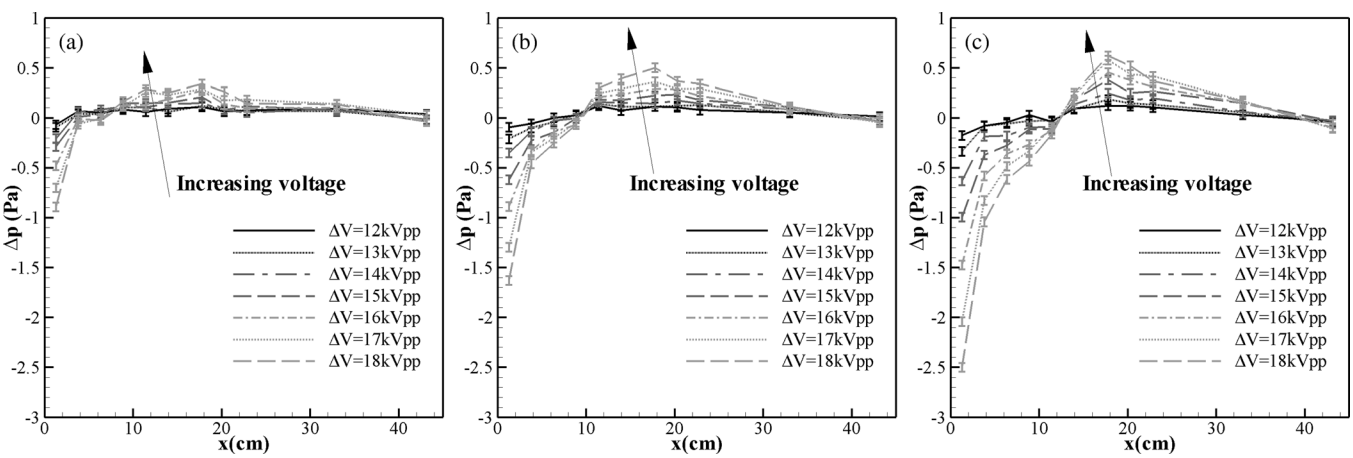

FIG. 10. Pressure measurements along the centerline and surface of the plasma channel for (a) 1, (b) 2, and (c) 3 actuators.

Downloaded 10 Sep 2012 to 128.227.210.184. Redistribution subject to AIP license or copyright; see http://jap.aip.org/about/rights_and_permissions

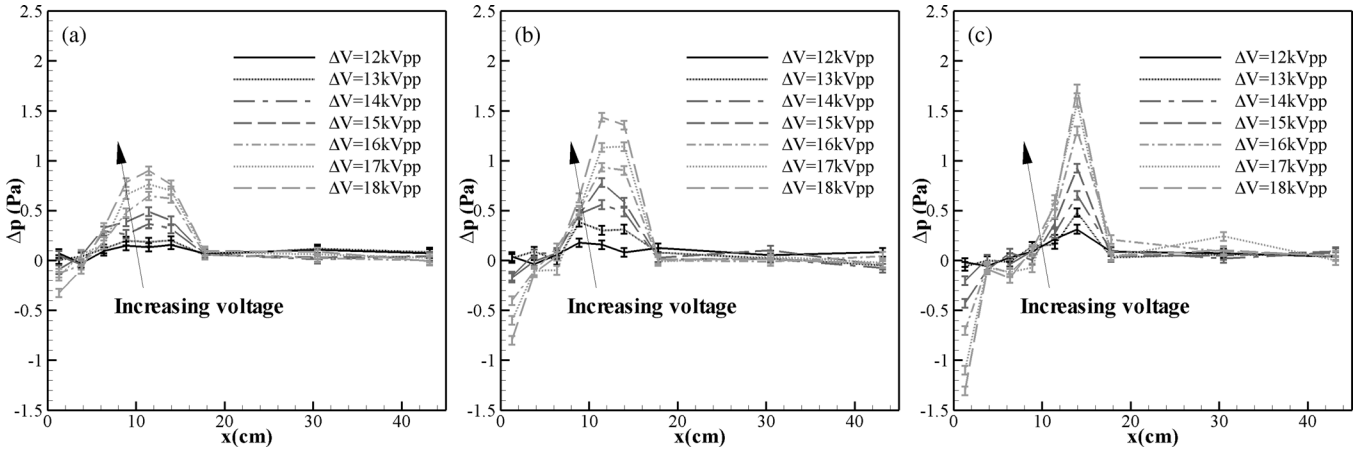

FIG. 11. Pressure measurements along the centerline and surface of the plasma channel with the addition of a screen impeding the channel flow for (a) 1, (b) 2, and (c) 3 actuators.

the thrust production, power consumption, and operating voltage of the plasma actuator. As such, a power law relationship is expected with the voltage. This leads to the approximate correlation

$$\Delta p_{max} \approx \alpha n_{act} V^{\beta}, \tag{2}$$

where α and β in Eq. (2) are the empirically derived constants $\alpha = 1.21 \times 10^{-7}$ and $\beta = 5.57$. In this relationship, the voltage V must be in kV_{pp}, the resulting pressure differential will be in Pascals.

Computational results as described above also show the increase in pressure around the plasma actuators. It is reiterated that the measurement of the centerline pressure from the simulations must be taken only qualitative in nature due to the uncertainties of the plasma models and the lack of transition the channel (Fig. 13).

However, a similar change in the pressure is seen for 1 through 3 actuators operated in the same locations as the experiments. It can be seen that the most significant drops occur at the locations of the plasma actuators, a similar gradual increase in the pressure downstream of the actuators, and eventually a slow drop in the pressure as the flow develops.

V. CHANNEL EFFICIENCY

Implementing these plasma actuators in a closed environment provides an opportunity to evaluate the efficiency of plasma actuators in imparting momentum to fluid in the channel. Defining this efficiency as the ratio of hydrodynamic power to the input electrical power

$$\eta = \frac{p_{flow}}{p_{in}} = \frac{\int_0^h u \Delta p dA}{p_{in}}, \tag{3}$$

which can be approximated in two different ways. If the average flow in Eq. (3) is assumed to be plug like, $u \approx u_{max}$, then the approximation becomes

$$\eta_u = \frac{u_{max} h \Delta p}{p_{in}/L}. \tag{4}$$

Equation (4) can also be considered an upper bound on the device efficiency. For a more accurate approximation using

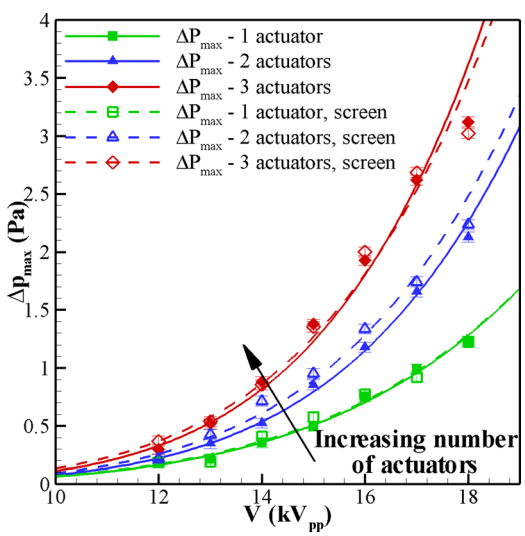

FIG. 12. Maximum pressure differential measured within the plasma channel. Solid and dashed lines denote power law curve fits to the data.

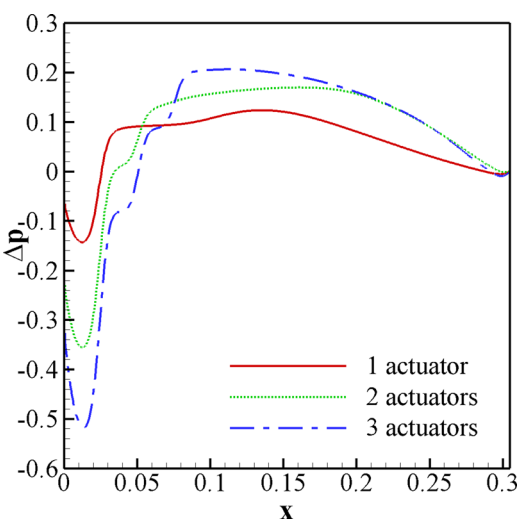

FIG. 13. Simulated pressure distribution along the channel for a varying number of plasma actuators.

Downloaded 10 Sep 2012 to 128.227.210.184. Redistribution subject to AIP license or copyright; see http://jap.aip.org/about/rights_and_permissions

the power and mass flow rate per unit width, the efficiency can be approximated as

$$\eta_Q = \frac{Q/w\Delta p}{p_{in}/w}. \tag{5}$$

Computing these efficiencies from Eqs. (4) and (5) using the experimental data (and using approximated data based on the power law curve fits when necessary), the efficiency of the plasma channel can be seen to be less that 0.1% (Fig. 14). The channel efficiency appears to be highly dependent on the operating voltage and increases an order of magnitude as the operating voltage is increased from a low to moderate value.

Using the different empirical power law relationships developed for u_{max}, Δp_{max}, and P_{in}, the efficiency of the channel can also be put in terms of a power law relationship with respect to the input voltage, such that

$$\eta_Q = \frac{(\alpha_Q n_{act}^{\gamma_Q} V^{\beta_Q})(\alpha_p n_{act} V^{\beta_p})}{(\alpha_e n_{act} V^{\beta_e})}, \tag{6}$$

$$\eta_Q = \frac{(\alpha_u n_{act}^{\gamma_u} V^{\beta_u})(\alpha_p n_{act} V^{\beta_p})}{(\alpha_e n_{act} V^{\beta_e})}, \tag{7}$$

where the various coefficients in Eqs. (6) and (7) are denoted by Q for the mass flow rate per unit width, and u for the maximum velocity, p for the maximum pressure, and e for the electrical input. α_e and β_e are the coefficients for the power law relationship for the electrical power input. Ignoring the constants, there is an important proportionality to these efficiency relationships.

$$\eta \approx \eta_{Q,u} \propto V^{\beta_{Q,u}+\beta_p-\beta_e}. \tag{8}$$

Computing this exponent in Eq. (8) based on the empirical curve fits, $\beta_Q + \beta_p - \beta_e = 4.35$ and $\beta_u + \beta_p - \beta_e = 4.09$, indicating that the plasma channel becomes increasingly more efficient at imparting momentum to the flow as the operating voltage is increased. However, the upper range of operating voltages is limited by the effects of plasma streamer formation and dielectric breakdown.[15]

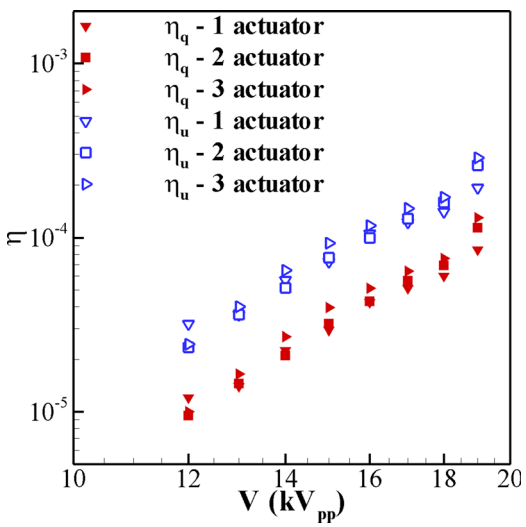

FIG. 14. Efficiency of the plasma actuation.

VI. CONCLUSIONS

The results of these experiments and simulations show that with the application of dielectric barrier discharge actuators, channel flows of up to several meters per second can be generated. In using DBD actuation to drive this flow, the actuation is effectively working as a low speed pump for small flows. A distinct difference exists as this type of pump is inherently two-dimensional in nature and can be extended to a very large width, something which traditional centrifugal and axial pumps cannot do. Furthermore, the present method of driving the flow differs from other electrodynamic methods as it can be applied to larger length scales.

The present work has discussed the results of experimental and numerical parametric studies varying the number of DBD actuators operated in a channel, as well as the operating voltage applied to these actuators. These experiments and simulations present the following conclusions:

(a) The exit velocities and maximum pressure, mass flux, and differential across an array of actuators fit well to a power law relationship with respect to the operating voltage. These relationships indicate that there is an increasing margin of return for the maximum velocities, mass flux, and pressure rise due to the actuators with respect to voltage. However, only the pressure differential continues to rise with respect to input electrical power as the voltage is increased. The maximum velocities and mass flux per unit power input decrease as the voltage is increased.

(b) Each plasma actuator generates the same pressure increase across its surface, independent of the bulk flow in the channel. While there may be some upper bound on the total pressure differential than can be created in the channel, the maximum pressure increase appears to have a linear relationship with the total number of actuators in the channel.

(c) Simulations of the flow show that in the absence of a laminar to turbulent transition mechanism, the channel flow is formed by the coalescing of symmetric wall jets created by DBD actuators in the channel. Furthermore, the trends in the pressure distribution and increases in the channel velocities as the number of actuators increases seen in the numerical simulations qualitatively agree with the experimental measurements.

(d) The efficiency of the DBD plasma channel can easily be inferred from the mass flow and maximum pressure differential in the channel. Using the previously developed power law relationships for the mass flow, maximum pressure differential, and electrical power input, the channel efficiency also appears to display a power law relationship with respect to the operating voltage, with an exponent on the order of 4.09 to 4.35. While the efficiency of the devices is low, this exponent suggests that large increases in efficiency may be possible.

Downloaded 10 Sep 2012 to 128.227.210.184. Redistribution subject to AIP license or copyright; see http://jap.aip.org/about/rights_and_permissions

While more characterization is necessary for various actuator geometries, the study indicates the possibility of using plasma actuators for pumping small flows within a channel.

ACKNOWLEDGMENTS

This work was sponsored in part by an AFOSR/DARPA grant, monitored by Dr. Doug Smith and Dr. David Barnhart. The views expressed are those of the authors and do not reflect the official policy or position of the Department of Defense of U.S. Government. The first author was also supported by the University of Florida Graduate School Fellowship Award.

[1]D. J. Laser and J. G. Santiago, "A review of micropumps," J. Micromech. Microeng. **14**, R35–R64 (2004).
[2]J. R. Roth, D. M. Sherman, and S. P. Wilkinson, "Boundary layer flow control with a one atmosphere uniform glow discharge surface plasma," AIAA Paper No. 98-328, 1998.
[3]T. C. Corke, C. L. Enloe, and S. P. Wilkinson, "Dielectric barrier discharge plasma actuators for flow control," Annu. Rev. Fluid Mech. **42**, 505–529 (2010).
[4]E. Moreau, "Airflow control by non-thermal plasma actuators," J. Phys. D: Appl. Phys. **40**, 605–636 (2007).
[5]C. C. Wang and S. Roy, "Three-dimensional simulation of a plasma micropump," J. Phys. D: Appl. Phys. **42**, 185206 (2009).
[6]J. C. Zito, R. J. Durscher, J. Soni, S. Roy, and D. P. Arnold, "Flow and force inducement using micro size dielectric barrier discharge actuators," Appl. Phys. Lett. **100**(19), 193502 (2012).
[7]M. Debiasi and L. Jium-Ming, "Experimental study of a DBD-plasma driven channel flow," AIAA Paper 2011-0954, 2011.
[8]D. Opaits, S. Zaidi, M. Shneider, A. Likhanskii, M. Edwards, and S. Macheret, "Surface plasma induced wall jets," AIAA Paper 2010-0469, 2010.
[9]W. G. Bickley, "The plane jet," Philos. Mag. **7**, 727 (1937).
[10]D. P. Rizzeta, M. R. Visbal, and P. E. Morgan, "A high-order compact finite-difference scheme for large-eddy simulations of active flow control," Prog. Aerosp. Sci. **44**, 397–426 (2008).
[11]K. P. Singh and S. Roy, "Force approximation for a plasma actuator operating in atmospheric air," J. Appl. Phys. **103**, 013305 (2008).
[12]W. Shyy, B. Jayaraman, and A. Andersson, "Modeling of glow discharge-induced fluid dynamics," J. Appl. Phys. **92**, 6434–6443 (2002).
[13]S. Roy, "Flow actuation using radio frequency in partially-ionized collisional plasmas," Appl. Phys. Lett. **86**(10), 101502 (2005).
[14]J. P. Boeuf, Y. Lagmich, T. Unfer, T. Callegar, and L. C. Pitchford, "Electrohydrodynamic force in dielectric barrier discharge plasma actuators," J. Phys. D: Appl. Phys. **40**, 652–662 (2007).
[15]F. O. Thomas, T. C. Corke, M. Iqbal, A. Kozlov, and D. Schatzman, "Optimization of dielectric barrier discharge plasma actuators for flow control," AIAA J. **47**(9), 2169–2178 (2009).

Downloaded 10 Sep 2012 to 128.227.210.184. Redistribution subject to AIP license or copyright; see http://jap.aip.org/about/rights_and_permissions